Structural, electronic and magnetic properties of P n+1 and FeP n (n = 1–14) clusters

S. Mahtout, N. Amatousse, Franck Rabilloud

Structural, electronic and magnetic properties of P_{n+1} and FeP_n (n=1-14) clusters

S. MAHTOUT[a], N. AMATOUSSE[a] and F. RABILLOUD[b]
[a]*Laboratoire de Physique Théorique, Faculté des Sciences Exactes, Université de Bejaia, 06000 Bejaia, Algérie.*
[b]*Univ Lyon, Université Claude Bernard Lyon 1, CNRS, Institut Lumière Matière, F-69622, Villeurbanne, France*
Corresponding authors: mahtout_sofiane@yahoo.fr, franck.rabilloud@univ-lyon1.fr

Abstract:

Density functional theory calculations have been performed to study the geometrical structures, relative stabilities, electronic and magnetic properties of P_{n+1} and FeP_n clusters in the range of n = 1 to 14 atoms. The search of the lowest-energy isomers has been performed by considering lots of structures for each clusters sizes. The putative geometries show that the frameworks of the lowest-energy isomers are three-dimensional structures and Fe atom tends to be located at an endohedral position from size n = 7. The growth pattern behaviors and relative stabilities are analyzed from the binding energies, second-order difference of energies, and HOMO-LUMO energy gaps. Doping with Fe atom enhances the stability of the P_n clusters. The HOMO-LUMO gaps are significantly affected after the introducing of a Fe atom into a phosphorus cluster. The vertical ionization potential (VIP), vertical electron affinity (VEA) and chemical hardness (η) are also calculated and discussed. The total spin magnetic moment analyses show that Fe atom can enhance dramatically the magnetic moment of the host cluster, but in some cases the magnetic moment is fully quenched. The total and partial density of states of clusters are discussed to understand the origin of these peculiar magnetic properties.

1. Introduction

During the last years, studies of small clusters have attracted a lot of interests, because of their specific physicochemical properties such as catalysis, optoelectronic responses, magnetism, and cluster assembled interfaces. It is very known that clusters properties may strongly be affected by the size, shape, or composition, and the matter at nanometric or subnanometric sizes is likely to behave differently than it does in bulk. Therefore there is a need to characterize the changes in structural, electronic and magnetic properties with the cluster size and cluster composition. But as the cluster size increases the number of possible isomers become very important so that searching for the lowest isomer is a very challenging task. [01]

It is very know that the bulk phosphorus shows several crystalline phases namely orthorhombic, pentagonal, rhombohedral and amorphous phase structures. The color and the properties of the phosphorus materials depend on these different phases. In the literature, numbers of theoretical and experimental studies on the pure and doped phosphorus clusters have been made and the evolutions of their properties have been discussed by several authors [02-26] because of their potential applications. Bare phosphorus and binary phosphide clusters have been generated from laser ablation and further investigated [02-06]. From the

theoretical point of view, most investigations have been performed using density functional theory (DFT) calculations. Amongst them, Wang et al. [07] have investigated very small phosphorus clusters P_n (n=1-6) with the DZP++ basis set, and they found that the structure of P_n clusters are planar for P_2 and P_3 in the neutral states and they are generally planar for all the anionic P_n clusters with size n=1-5. Neutral, cationic and anionic P_n (n=5, 7, 9) clusters are given by Chen et al. [08] by using the hybrid exchange and correlation functional B3LYP. They found that the cationic cluster prefers the structure with P atoms in four-fold coordination and the planar pentagonal structure is a common unit in phosphorus clusters. Using the PM3 semi-empirical method and DFT calculations in the search for isomers of neutral P_8 and cationic P_9, Chen et al. [10] have showed that the tridimensional cage-shape structures are more stable than the planar ones while the structures with a large planar ring are poorly stable. Han and Morales [11] showed that fullerene-like phosphorus clusters are unstable with respect to dissociation into P_4. The ground-state structures of neutral, cationic, and anionic phosphorus clusters in the range size of n= 2 to 15 atoms have been investigated at DFT level [03,09], and it was found that in the anionic and cationic states, the clusters with odd number of atoms are more stable than those with even number of atoms, while the most stable clusters in neutral systems are even-numbered. Heterogeneous clusters containing phosphorous atoms have already been considered in previous works. Among them, one can found In_nP_n [12], N_nP_m [13], C_nP_m, Si_nP_m, B_nP_m, Al_nP_m [06]. Aluminum phosphides have been more intensively investigated. In their different contributions, Guo et al. [14-16] have investigated the structures and stability of a number of isomers of small Al_nP_m clusters in the neutral, cationic and anionic states at DFT level and they showed that singlet structures have higher symmetries than those of doublet structures. In a more recent work on the structural and electronic properties of AlP_n ($2 \leq n \leq 12$) clusters, Guo [17] have showed that the lowest-energy geometries for AlP_n clusters favor a peripheral position for Al, while AlP_5 and AlP_7 are found to have relative high stabilities. The effects of P substitutions on the octahedral Fe cluster have been recently investigated at DFT level and it was shown that the change in binding energies is due to the charge transfer from Fe to P atoms [18].

Despite of numbers of previous studies, most of the studies on the P_n clusters have been focused on searching for the lowest-energy structures of very small clusters (n<10) and less effort has been devoted to larger size clusters. On the other hand and to the best of our knowledge, a systematic investigation of the phosphorus clusters doped by transition metal Fe atoms has not been reported yet. In the present work, we systematically investigate the structural, electronic and magnetic properties of P_{n+1} and FeP_n clusters, in the range of size n=1 to n=14 atom, by using first principles calculations. In order to explore the physical and chemical properties such as catalysis, electronic and magnetic behavior, it is first very important to obtain the best geometrical structures of phosphorus and transition metal Fe doped phosphorus clusters. Our attention is focused on the geometric structures and the size-dependence of the stability, electronic and magnetic properties of bare and iron doped phosphorus clusters. We first explore the equilibrium geometries, binding energies and electronic properties of pure P_{n+1} clusters (n = 1-14). Then, we examine the influence of the substitution of one P atom by one Fe atom on the clusters properties. In the next section, we give a brief description of the theoretical method and computational details. Results and discussions are presented in section 3.

2. Computational details

Calculations were performed with *ab initio* density functional theory calculations implemented in SIESTA package [27] to find the lowest-energy structure for a given cluster size. The SIESTA code uses a localized numerical pseudo-atomic orbitals basis set and norm-conserving pseudopotentials. Here we used the norm conserving Troullier-Martins pseudopotentials type [28] with a double zeta ζ (DZ) basis set for P atoms and a double zeta ζ with polarization function (DZP) basis set for Fe atom. The generalized gradient approximation formulated by Perdew, Burke, and Ernzerhof (PBE) is used for the exchange correlation energy functional [29]. All calculations were spin-polarized. We used a convergence criterion of 10^{-4} Hartree on the total energy for the self-consistent field calculations. A large cubic cell of 40 Å edge lengths with a periodic boundary condition is taken in order to avoid interactions between neighboring clusters and the Γ point approximation for the Brillouin zone sampling is considered. The total spin magnetic moments of these structures were obtained by Mulliken population analysis.

Geometry relaxations were performed using the conjugated gradient method and without any symmetry constraints. The number of geometric isomers or local minima increases exponentially with the cluster size. For this reason, lots of putative isomers including some high and low symmetries were relaxed for each cluster size. Amongst them, some initial structures of P_{n+1} and metal-doped P_n clusters were taken from literature. Also, the putative structures of FeP_n were obtained by local relaxation after the substitution of one P atom by Fe atom in several isomers of the original pure P_{n+1} cluster. The different initial positions of the P atom in the P_{n+1} clusters lead to different FeP_n isomers. But the search for the lowest isomer cannot include a global optimization procedure of the potential energy surface, and we cannot be sure that a more stable structure than those found in our calculations does not exist. In the next section, we only show the best calculated structures for each cluster size.

The validity of current computational method was tested on Fe_2 and P_2 dimers as benchmark systems. The obtained results, reported in table 1, show good agreement with available calculated and experimental data.

3. Results and discussions

3.1. Structural analysis

By using the computation scheme described above, we have explored a number of isomers and determined the lowest energy structures for P_{n+1} and FeP_n clusters with n = 1-14 atoms. The obtained structures are shown in Fig 01 and Fig 02. Symmetry and others physical data of the different structures of P_{n+1} and FeP_n (n = 1-14) clusters are summarized in Table 2 and 3 respectively. In the present level of calculation, the P_2 dimer has an equilibrium bond distance of 1.944 Å and binding energy of 1.979 eV per atom. Our results are very close to those obtained in other previous theoretical calculations [07, 09]. Our calculated equilibrium distance of 1.944 Å slightly overestimates the experimental data of 1.893 Å (Table 1).The FeP dimer with a bond length of 2.126 Å and a binding energy of 1.352 eV is less stable than the P_2 dimer.

The comparison between P_{n+1} and FeP_n clusters highlights a structural reconstruction following the substitution of a P atom by a Fe atom since the doping atoms tends to maximize the number of bonds. In the case of P_n clusters with n=3-5, our results are in good agreement with those of reported by Wang et al. [07] and Guo et al. [09], namely a linear structure for P_3,

the tetrahedral triangular pyramid structure with T_d symmetry for the tetramer P_4 and a distorted rectangular pyramid structure with C_{2v} symmetry for P_5 cluster. The most stable structure of the trimer FeP_2 is an isosceles triangle in which the single Fe atom occupies the apex angle of 59.5° while the identical Fe-P bonds length are 2.227 Å. The Fe-P bond length is slightly less than the P-P bond legth 2.201 Å in the corresponding P_3 cluster. In the case of FeP_3 tetramer, the most stable structure is the tridimensional butterfly structure (labeled a in Fig 3) with C_s symmetry. The Fe-P bond distance of 2.186 Å is shorter than the P-P bond distance of 2.382 Å observed in the corresponding P_4 cluster. In the case of FeP_4 clusters, the capped butterfly structure with C_s symmetry is the most stable. The average Fe-P bond distance of 2.184 Å is shorter than the P-P bond distance of 2.429 Å. The significant reduction in the bond length when P is substituted by Fe and the valence orbitals interactions of Fe with the neighboring P atoms leads to a stronger stability. A cuneane-like structure with C_{2v} symmetry is the most stable in the case of P_6 clusters. However, this structure is no longer stable when a P atom is substituted by a Fe atom. The most stable isomer of FeP_5 cluster consists of a pentagonal pyramid structure with C_{5v} symmetry where the Fe atom occupies the top position on the pentagonal plane bases formed by the P atoms. The calculated average P-P and Fe-P bond distances are 2.340 Å and 2.347 Å respectively.

From n=6 to n=14, the Fe atom is found to occupy a central position and to be highly coordinated to the neighboring P atoms so that the most stable isomer of FeP_n strongly differs from the counterpart P_{n+1} and can be seen as an open or closed cage where Fe is encapsulated inside a phosphorus cage. A tridimensional distorted hexagonal structure with Fe atom located at the center of a P_6 skeleton is the ground-state isomer of FeP_6 clusters. Its point group symmetry is C_2. The average Fe-P and P-P bond lengths are 2.389 and 2.498 Å respectively. A more compact structure with three distorted pentagonal faces and a Fe atom highly coordinated located at the center of P_7 cage is obtained for FeP_7 clusters. Its point group symmetry is C_{3v}. The ground state structure of FeP_8 is formed by two pentagons of P atoms with a highly coordinated Fe atom at the top of the structure. It belong C_{2v} point group symmetry. In the case of FeP_9 a multiface pentagonal structure with C_1 symmetry is obtained. The Fe atom which occupies a center of pentagon face are highly coordinated with 7 neighboring P atoms. The corresponding most stable pure P_{10} cluster presents a prolate-like structure and C_{2v} symmetry. From n=10 to n=12, the ground states isomers of FeP_{10}, FeP_{11} and FeP_{12} clusters show somewhat similar structures where two subunits of P atoms are linked by a central highly coordinated Fe atom. They significantly differ from the counterparts P_{11}, P_{12} and P_{13} clusters that present a prolate-like structure without any core atoms. In the case of FeP_{13} cluster, a like spherical structure with Fe atom located inside a P_n cage is obtained. The best isomer of the P_{14} cluster is constituted by a multifaceted pentagonal blocs without core atoms. A prolate-like structure with a central Fe atom highly coordinated and a C_{2v} symmetry is obtained for FeP_{14} cluster.

3.2. Relative stability and electronic properties

In order to understand the relative stability of P_{n+1} and FeP_n clusters, we present the average binding energy per atom and the second-order differences of energies. The average binding energies are obtained by the following formulas:

$$E_b(P_{n+1}) = ((n+1)\,E(P) - E(P_{n+1}))\,/\,(n+1),$$
$$E_b\,(FeP_n) = (n\,E(P) + E(Fe) - E(FeP_n))\,/\,(n+1),$$

where E(P) and E(Fe) are the single atom energies for P and Fe, and E(P_{n+1}) and E(FeP_n) are the total energies for P_{n+1} and FeP_n, respectively. The obtained results are summarized in tables 2 and 3. The size dependence for the lowest energy structures is shown in Fig. 03. It can also be seen that the average binding energies of P_{n+1} and FeP_n clusters globally increase with cluster size. This means that these clusters can continuously gain energy during the growth process. The doping Fe atom in the P_n clusters significantly enhances the stability of the phosphorus framework. A pronounced peaks in the binding energies of FeP_n clusters are observed at n = 5, 8 and 11 implying that these clusters are more stable than the others.

The second-order energy difference (Δ_2E) of the cluster total energy is a sensitive parameter that reflects the relative stability of clusters. Experimentally it can be directly compared to the relative abundance of the corresponding cluster in mass spectroscopy experiments. The Δ_2E value was calculated by using the following formulae:

$$\Delta_2E\ (P_{n+1}) = E(P_{n+2}) + E(P_n) - 2E(P_{n+1}),$$
$$\Delta_2E(FeP_n) = E(FeP_{n+1}) + E(FeP_{n-1}) - 2\,E(FeP_n),$$

where *E* is the total energy of the relevant systems. The obtained results are plotted in Fig. 04. Neutral phosphorus clusters with even number of atoms are most stable than clusters with odd number of atoms, consistently with the even-odd alternation measured in mass spectra [04, 06]. In contrast, the even-odd alternation is no longer observed for FeP_n cluster, but pronounced positive peaks of Δ_2E are obtained at n = 5, 8 and 11, indicating these clusters have special stability compared to the others.

The vertical ionization potential (VIP) is also a good parameter that can characterize the stability of small clusters and could be compared to experiment even if to our knowledge no experimental data are available nowadays. The VIP is defined as:

$$VIP = E^+ - E$$

where E is the total energy of the neutral cluster and E^+ is the total energies of the cationic clusters respectively with the same geometry as the corresponding neutral cluster. In Fig. 05 we show the size dependence of VIP for the most stable P_{n+1} and FeP_n clusters. A very large value is observed for pure P_3, then the VIP of P_{n+1} shows an oscillating behavior and a decreasing tendency. For FeP_n clusters, VIP shows a smaller size dependence even if a higher value is observed at n=3, 5, 8. From n = 11, VIP shows a slow tendency to increase with n, and FeP_{14} has a higher VIP than Fe_{15}.

The vertical electron affinity (VEA) is the difference in the energy between the anionic and neutral clusters, both calculated at the geometry of the neutral species. The obtained VEA for the ground state structures of P_{n+1} and FeP_n clusters are shown in Fig. 06. In chemical reactivity, large values of electron affinity mean that the corresponding clusters are likely to accept an electron. For P_{n+1} clusters, our calculated VEA values are usually found to be 0.3−0.8 eV smaller than the experimental electron detachment energies of the anion P_n^- [02]. We observe an odd-even alternation, except for n=5, and an increasing tendency as a function of the size. The clusters with odd number of atoms have higher VEA than those with even number of atoms. This means that the clusters with even number of atoms become less stable after it acquired an electron comparatively to the clusters with odd numbers of atoms. For FeP_n clusters the VEA increases with the increasing *n*. Adding an electron to a very small

FeP_n clusters will lead to a strong instability, while larger (n>8) clusters have a high VEA of about 3 eV or higher.

The Chemical hardness is a quantity that can characterizes the relative stability of clusters. It is calculated from VIP and VEA values for each cluster according to the definition of hardness of Parr and Pearson [41, 42]. The chemical hardness η is defined as:

$$\eta = VIP\text{-}VEA.$$

Values of η for all P_{n+1} and FeP_n clusters are summarized in Table 2 and 3 and its evolution for the lowest-energy structures are plotted in Fig. 07. Local maxima of chemical hardness appear for odd values of n for pure P_{n+1} clusters, indicating that the phosphorus clusters with even number of atoms are more stable and less reactive than their neighboring with odd number of atoms. In cases of FeP_n clusters, FeP_3, FeP_5 and FeP_8 show a relative high stability comparing to the other sizes.

The cluster which has a large gap between the highest occupied molecular orbital (HOMO) and lowest unoccupied molecular orbital (LUMO) have the high chemical stability. We have calculated the HOMO-LUMO gap as the minimum energy between the gap for alpha electrons and the gap for beta electrons. For both P_{n+1} and FeP_n clusters, the evolution of the HOMO-LUMO gaps with the size is shown in Fig. 08. While the gaps of P_{n+1} show a strong dependence of the cluster size, those of FeP_n clusters present a much more regular behavior. Pronounced peaks are found at n = 3, 7, 11 and 13 for pure phosphorus clusters and at n= 5, 8, 10 and 12 for iron doped phosphorus clusters suggesting a relative high chemical stability for these clusters.

3.3. Magnetic properties

In this section we describe the magnetic properties of the P_{n+1} and FeP_n clusters on the basis of the total spin magnetic moment and the partial density of states (PDOS). The obtained total spin magnetic moments for all clusters are reported in table 2 and Table 3. In Fig. 09, we compare the total spin magnetic moments of the most stables structures of both P_{n+1} and FeP_n clusters. Magnetic moments of the pure phosphorus clusters show a perfect odd-even behavior since the clusters with even number of P atoms exhibit nonmagnetic moment while the clusters with odd number of P atoms have a total spin magnetic moment of 1 μ_B. As expected the magnetic moments are stronger for iron doped clusters. The total magnetic moment is maximum for FeP_4 and FeP_{10} with the value of 4 μ_B. As a matter of fact it is the value of the isolated Fe atom. However the total magnetic moment is quenched in FeP_7 and FeP_{13} with the minimal value of 1 μ_B. In these structures, Fe is totally encapsulated inside a closed cage. Interestingly, there is clear correlation between the total magnetic moment and the surrounding of Fe. The more Fe is surrounded by phosphorus atoms, the more the magnetic moment is quenched.

In order to explain the real origin of the total spin magnetic moment of different species we explore the contribution of valence orbitals to the total magnetic moment by analyzing of their partial density of states (PDOS). We report in Fig. 10 the projected density of states of the lowest energy structures of P_2, P_3, FeP_1, FeP_4 and FeP_7 clusters. As we can see, there is no magnetic moment due to the valence orbital in phosphorus P_2 clusters. This

behavior is observed for all the clusters with even number of atoms. However, in the P_3 cluster, the total spin magnetic moment is mainly due to the 3p orbital. In the case of FeP_n clusters, we first examine the FeP_4 cluster with presents a high value of magnetic moment. For better understanding the contribution of each species, we show separately the contribution of each species to the total spin magnetic moment in Fig. 10. We observe that the total spin magnetic moment of FeP_4 cluster is mainly originated from the 4d state of Fe atom, with small contributions from the 3p of P atoms and 4s of Fe atom. In contrary, in the case of FeP_7 clusters, we observe that there is no contribution of Fe atom to the total magnetic moment. This means that the spin magnetic moment of Fe atom, which is located at the center of the cluster, is completely quenched by the P_n cage. This should be due to orbital hybridizations and charge transfers. Interestingly, the smallest value of 1 μ_B is due to the 3p orbital of P atoms. The same behavior is observed for FeP_{13} cluster where the Fe atom is located at the center of P_n cage.

4. Conclusion

Ab initio calculations in the framework of density functional theory have been performed to study the geometries, stabilities, and electronic and magnetic properties of P_{n+1} and FeP_n (n=1=14) clusters. The lowest-energy structures and some low-lying isomers have been identified for both pure and iron doped phosphorus clusters. The lowest-energy structures of iron doped clusters significantly differ from those of bare phosphorus clusters since GeP_n clusters usually adopt endohedral structures where Fe is surrounded by P atoms, leading to open or closed cagelike structures. Relative stabilities were analyzed tanks to binding energies, second-order difference of energies, and HOMO-LUMO energy gaps. Ionization potentials, vertical electron affinities and chemical hardness were also calculated and discussed. The substitution of a P atom by a Fe atom usually enhances the magnetic moment of the host cluster, but in some cases the magnetic moment is fully quenched (FeP_7 and FeP_{13}). The total (DOS) and partial (PDOS) density of states of clusters was discussed to understand the origin of these peculiar magnetic properties.

Our theoretical study gives important information for better understanding the influence of a transition metal Fe atom and the change on the properties of small systems of phosphorus. We hope that the relevant information will provide strong motivation for further experimental and theoretical researches.

Acknowledgments
The Pôle Scientifique de Modélisation Numérique at Lyon, France, and the GENCI-IDRIS (Grant No. i2016086864) center are thanked for generous allocation of computational time.

References

[01] Alonso J A, Structure and Properties of Atomic Nanoclusters, Imperial College Press; 2nd edition (August 23, 2011).

[02] Jones R O, Gantefor G, Hunsicker S, Pieperhoff P, Structure and spectroscopy of phosphorus cluster anions: Theory (simulated annealing) and experiment (photoelectron detachment), 1995 *J. Chem. Phys.* **103** 9549-9562.

[03] Chen M D, Chen Q B, Liu J, Zheng L S, Zhang Q E, Parity Alternation of Ground-State P_n^- and P_n^+ (n = 3-15) Phosphorus clusters, 2007 *J. Phys. Chem. A* **111** 216-222.

[04] Bulgakov A V, Bobrenok O F, Kosyakov V I, Laser ablation synthesis of phosphorus clusters, 2000 *Chem. Phys. Lett.* **320** 19-25.

[05] Yang S, Mu L, Kong X, Collision-induced dissociation mass spectrometry of phosphorus cluster anions $P^{-2}_{m+1}(3 \leq m \leq 20)$, 2016 *Int. J. Mass Spec.* **399-400** 27-32.

[06] Liu Z Y, Huang R B, Zheng L S, Bare phosphorus and binary phosphide cluster ions generated by laser ablation, 1996 *Z. Phys. D* **38** 171-177.

[07] Wang D, Xiao C, Xu W, The phosphorus clusters P_n (n=1-6) and their anions: Structures and electron affinities, 2006 *J. Mol. Struct.: THEOCHEM* **759** 225-238.

[08] Chen M D, Huang R B, Zheng L S, Zhang Q E, Au C T, A theoretical study for the isomers of neutral, cationic and anionic phosphorus clusters P_5 , P_7 , P_9, 2000 *Chem. Phys. Lett.* **325** 22-28.

[09] Guo L, Wu H, Jin Z, First principles study of the evolution of the properties of neutral and charged phosphorus clusters, 2005 *J. Mol. Struct.: THEOCHEM* **677** 59-66.

[10] Chen M D, Huang R B, Zheng L S, Au C T, The prediction of isomers for phosphorus clusters P_8 and P_{19}, 2000 *J. Mol. Struct.: THEOCHEM* **499** 195-201.

[11] Han J G, Morales J A, A theoretical investigation on fullerene-like phosphorus clusters, 2004 *Chem. Phys. Lett.* **396** 27-33.

[12] Wanga L, Zhao J, Lowest-energy structures and photoelectron spectra of In_nP_n (n = 1-12) clusters from density functional theory, 2008 *J. Mol. Struct. THEOCHEM* **862** 133-137.

[13] Valadbeigi Y, Phosphorus-doped nitrogen clusters (N_nP_m): Stable high energydensity materials, 2016 *Chem. Phys. Lett.* **645** 195-199.

[14] Guo L, Wu H, Jin Z, Ab initio investigation of structures and stability of Al_nP_m clusters, 2004 *J. Mol. Struct.: THEOCHEM* **684** 67-73.

[15] Guo L, Wu H, Jin Z, First principles study of the structure, electronic state and stability of $Al_nP_m^+$ cations, 2004 *J. Mol. Struct.: THEOCHEM* **680** 121-126.

[16] Guo L, Wu H, Jin Z, First principles study of the structure, electronic state and stability of $Al_nP_m^-$ anions, 2004 *J. Mol. Struct.: THEOCHEM* **683** 43-50.

[17] Guo L, Density Functional Study of Structural and Electronic Properties of AlP_n ($2 \leq n \leq 12$) Clusters, 2013 *J. Clust. Sci.* **24** 165-176.

[18] Nakazawa T, Igarashi T, Tsuru T, Kaji Y, Jitsukawa S, Density functional calculations for small iron clusters with substitutional phosphorus, 2011 *J. Nucl. Mat.* **417** 1090-1093.

[19] Feng J N, Cui M, Huang X R, Otto P, Gu F L, Calculated properties of cationic phosphorus clusters P_{2n+1}^+ with n = 3, 4, 5, and 6, 1998 *J. Mol. Struct.: THEOCHEM*, **425** 201-206.

[20] Huang R, Li H, Lin Z, Yang S, Experimental and Theoretical Studies of Small Homoatomic Phosphorus Clusters, 1995 *J. Phys. Chem.* **99** 1418-1423.

[21] Andrews L, Mielket Z, Vibronic Absorption Spectra of P_4^+ and P_3 in Solid Argon, 1990 *J. Phys. Chem.* **94** 2348-2350.

[22] Hiiser M., Schneider U, Ahlrichs R, Clusters of Phosphorus: A Theoretical Investigation, 1992 *J. Am. Chem. Soc.* 114 9551-9559.

[23] Chen M D, Li J T, Huang R B, Zheng L S, Au C T, Structure prediction of large cationic phosphorus clusters, 1999 *Chem. Phys. Lett.* **305** 439-445.
[24] Nava P, Ahlrichs R, Theoretical Investigation of Clusters of Phosphorus and Arsenic: Fascination and Temptation of High Symmetries, 2008 *Chem. Eur. J.* **14** 4039-4045.
[25] Chen M D, Li J T, Huang R B, Zheng L S, Au C T, Structure prediction of large cationic phosphorus clusters, 1999 *Chem. Phys. Lett.* **305** 439-445.
[26] Kuang X, Wang X, Liu G, Geometrical structures and probable dissociation channels of CrP_m^+ (m=2, 4, 6, 8) clusters, 2010 *Physica B* **405** 3328-3333.
[27] Ordejón P, Artacho E and Soler J M, 1996 *Phys. Rev. B (Rapid Comm.)* **53**, 10441; Soler J M, Artacho E, Gale J D, García A, Junquera J, Ordejón P, and Sánchez-Portal D, 2002 *J. Phys.: Condens. Matt.* **14**, 2745.
[28] Troullier N and Martins J L, Efficient pseudopotentials for plane-wave calculations, 1991 *Phys. Rev. B* **43** 1993.
[29] Perdew J P, Burke K, and Ernzerhof M, Generalized Gradient Approximation Made Simple, 1996 *Phys. Rev. Lett.* **77** 3865-3868.
[30] Brassington N J, Edwards H G M, Long D A, The vibration-rotation Raman spectrum of P_4 , 1981 *J. Raman Spectrosc.* **11** 346-348.
[31] Huber K P, Herzberg G, Molecular Spectra and Molecular Structure IV. Constants of Diatomic Molecules, Van Nostrand Reinhold, New York (1979).
[32] Nakazawa T, Igarashi T, Tsuru T, Kaji Y, Ab initio calculations of Fe-Ni clusters, 2009 *Comp. Mat. Sci.* **46** 367-375.
[33] Harris J, Jones R O, Density functional theory and molecular bonding. III. Iron-series dimers, 1979 *J. Chem. Phys.* **70** 830-841.
[34] Cheng H P, Ellis D E, Electronic structure, binding energies, and interaction potentials of transition metal clusters, 1991 *J. Chem. Phys.* **94** 3735-3747.
[35] Ballone P, Jones R O, Structure and spin in small iron clusters, 1995 *Chem. Phys. Lett.* **233** 632-638.
[36] Noro T, Ballard C, Palmer M H, Tatewaki H, The ground state of the Fe_2 molecule, 1994 *J. Chem. Phys.* **100** 452-458.
[37] Cervantes-Salguero K, Seminario J M, Structure and energetics of small iron clusters, 2012 *J Mol. Mod.* **18** 4043-4052.
[38] Liang X Q, Deng X J, Lu S J, Huang X M, Zhao J J, Xu H G, Zheng W J, Zeng X C, Probing Structural, Electronic, and Magnetic Properties of Iron-Doped Semiconductor Clusters $Fe_2Ge_n^{-1/0}$ (n = 3-12) via Joint Photoelectron Spectroscopy and Density Functional Study, 2017 *J. Phys. Chem. C* **121** 7037−7046.
[39] Montano P A, Shenoy G K, EXAFS study of iron monomers and dimers isolated in solid argon, 1980 *Solid State Commun.* **35** 53-56.
[40] Purdum H, Montano P A, Shenoy G K, Morrison T, Extended-x-ray-absorption-fine-structure study of small Fe molecules isolated in solid neon, 1982 *Phys. Rev. B* **25** 4412-4417.
[41] Parr R G, Yang W, Density functional theory of atoms and molecules. New York: Oxford University Press (1989).
[42] Parr R G, Pearson R G, Absolute hardness: companion parameter to absolute electronegativity. 1983 *J. Am. Chem. Soc.* **105** 7512e6.

Table 1 Bond length (Å) of P_2 and Fe_2 dimers: comparisons with other available experimental and theoretical data.

Dimer	Our work	Theoretical value	Experimental value
P_2	1.944	1.874-1.923 [a], 1.90 [b],	1.893 [c], 1.890 [d]
Fe_2	2.126	2.15 [e], 2.10 [f], 2.22 [g], 2.06 [h, i] 2.003[j], 2.04[k]	1.87 [l], 2.02±0.2 [m]

[a] Ref. [07].
[b] Ref. [09].
[c] Ref. [30].
[d] Ref. [31].
[e] Ref. [32]
[f] Ref. [33]
[g] Ref. [34]
[h] Ref. [35]
[i] Ref. [36].
[j] Ref. [37].
[k] Ref. [38].
[l] Ref. [39].
[m] Ref. [40].

Table 2 Symmetry group, Binding energy per atom E_b (eV/atom), HOMO-LUMO gap *ΔE(eV)*, total spin magnetic moments μ (μ_B), Vertical Ionization Potential *(VIP) (eV)*, Vertical Electronic Affinity *(VEA) (eV)*, and Chemical Hardness η (eV) for P_{n+1} (n=1-14) clusters.

Cluster	Symmetry	E_b(eV/atom)	*ΔE (eV)*	μ (μ_B)	VIP (eV)	VEA (eV)	η (eV)
P_2	$D_{\infty h}$	1.979	3.416	0.000	10.723	0.198	10,525
P_3-a	C_{2v}	1.579	1.711	3.000	7.797	1.949	5,848
P_3-b	$D_{\infty h}$	**1.610**	**2.160**	**1.0000**	**7.999**	**2.471**	**5,528**
P_4-a	D_{4h}	1.875	0.923	2.000	8.883	2.571	6,312
P_4-b	C_{2v}	1.9223	1.932	2.000	8.350	1.850	6,500
P_4-c	T_d	**2,246**	**4.434**	**0.000**	**9.678**	**0.433**	**9.245**
P_5-a	C_{2v}	**2.120**	**1.847**	**1.000**	**8.048**	**1.778**	**6,270**
P_5-b	C_s	1.897	0.131	1.000	7.630	2.823	4,807
P_6-a	D_2	2.281	2.015	0.000	9.175	2.327	6,848
P_6-b	C_{2v}	**2.316**	**1.546**	**0.000**	**8.574**	**1.918**	**6,656**
P_7-a	C_1	**2.280**	**1.134**	**1.0000**	**8.239**	**2.866**	**5,373**
P_7-b	C_s	2.252	0.911	1.000	8.419	3.020	5.399
P_7-c	C_{2v}	2.219	1.288	1.000	8.319	2.438	5.881
P_8-a	O_h	2.252	1.545	0.000	8.243	2.081	6.162
P_8-b	C_s	2.346	1.738	0.000	8.540	2.009	6.531
P_8-c	**C_{2v}**	**2.413**	**2,087**	**0.000**	**8,431**	**1.713**	**6.718**
P_8-d	D_{3d}	2.250	4.110	0.000	8.701	0.558	8.143
P_9-a	C_1	**2.326**	**1.072**	**1.000**	**7.985**	**2.825**	**5.160**
P_9-b	C_s	**2.328**	**1.056**	**1.000**	**7.925**	**3.054**	**4.871**
P_9-c	C_1	2.300	1.113	1.000	8.112	3.023	5.089
P_9-d	C_1	2.238	1.209	1.000	8.049	2.532	5.517
P_{10}-a	C_{2v}	2.294	2.183	0.000	8.050	1.803	6.247
P_{10}-b	C_s	2.383	2.199	0.000	8.362	1.961	6.401
P_{10}-c	C_1	2.377	1.456	0.000	8.347	2.461	5.886
P_{10}-d	C_{2v}	**2.442**	**0.372**	**0.000**	**8.381**	**1.662**	**6.719**
P_{10}-e	C_s	2.210	0.916	4.000	7.929	3.356	4.573
P_{10}-f	C_s	2.303	1.978	0.000	8.561	2.553	6.008
P_{10}-g	C_1	2.377	1.453	0.000	8.348	2.466	5.882
P_{11}-a	C_1	**2.390**	**0.954**	**1.000**	**7.997**	**3.037**	**4.960**
P_{11}-b	C_1	2.383	1.046	1.000	7.743	3.506	4.237
P_{11}-c	C_1	2.353	1.365	1.000	7.879	2.728	5.151
P_{12}-a	D_{6h}	2.311	1.150	0.000	7.700	2.636	5.064
P_{12}-b	C_s	2.240	0.625	2.000	7.243	3.413	3.830
P_{12}-c	C_s	2.392	1.825	0.000	8.311	2.433	5.878
P_{12}-d	C_2	2.370	0.450	0.000	7.923	3.461	4.462
P_{12}-e	C_{2v}	**2.441**	**2.063**	**0.000**	**8.219**	**2.111**	**6.108**
P_{12}-f	C_{2h}	2.433	2.263	0.000	8.196	2.054	6.142
P_{13}-a	C_1	2.406	0.713	1.000	7.886	3.254	4.632
P_{13}-b	C_{2v}	2.233	0.475	0.001	7.088	3.252	3.836
P_{13}-c	C_1	2.336	0.646	0.006	7.298	3.315	3.983
P_{13}-d	C_{2v}	2.239	0.513	5.000	7.591	3.540	4.051
P_{13}-e	C_s	**2.445**	**0.552**	**1.000**	**7.786**	**3.325**	**4.461**
P_{13}-f	C_s	2.384	0.935	1.000	7.890	3.102	4.788
P_{14}-a	C_1	2.407	1.580	0.000	7.769	2.258	5.511
P_{14}-b	C_s	**2.439**	**1.896**	**0.000**	**8.027**	**2.298**	**5.729**
P_{14}-c	D_{3h}	2.422	1.759	0.000	8.040	2.521	5.519
P_{14}-d	D_{2h}	2.369	1.119	0.000	7.976	3.017	4.959
P_{14}-e	C_1	2.410	0.747	2.000	7.816	3.491	4.325
P_{14}-f	C_1	2.177	1.025	3.995	7.121	3.241	3.880
P_{15}-a	C_s	2.388	0.970	1.000	7.790	3.083	4.707
P_{15}-b	C_1	2.406	0.878	1.000	7.921	3.336	4.585
P_{15}-c	C_{2v}	2.446	0.161	0.910	7.815	4.034	3.781
P_{15}-d	C_1	2.440	1.008	1.000	7.697	3.258	4.439
P_{15}-e	C_1	**2.463**	**0.821**	**1.000**	**7.727**	**3.407**	**4.320**

Table 3 Symmetry group, Binding energy per atom E_b (eV/atom), total spin magnetic moments μ (μ_B), HOMO-LUMO gap ΔE(eV), Vertical Ionization Potential (VIP) (eV), Vertical Electronic Affinity (VEA) (eV), and Chemical Hardness η (eV) for FeP_n (n=1-14) clusters.

Cluster	Symmetry	E_b (eV)	μ (μ_B)	ΔE (eV)	VIP (eV)	VEA (eV)	η (eV)
FeP_1	$C_{\infty v}$	1.352	5.000	1.172	7.769	0.960	6.809
FeP_2-a	**C_{2v}**	**2.0452**	**2.000**	**0.757**	**6.854**	**0.704**	**6.150**
FeP_2-b	$D_{\infty h}$	1.374	8.000	0.845	7.926	2.488	5.439
FeP_3-a	**C_s**	**2.290**	**3.000**	**0.923**	**7.884**	**1.416**	**6.469**
FeP_3-b	C_1	2.071	5.000	0.462	7.706	2.579	5.126
FeP_3-c	C_{3v}	2.164	5.000	0.900	7.341	1.254	6.087
FeP_4-a	C_{4v}	2.387	4.000	1.168	8.171	1.511	6.660
FeP_4-b	C_{2v}	2.390	2.000	0.482	7.723	2.427	5.297
FeP_4-c	**C_s**	**2.417**	**4.000**	**1.008**	**7.641**	**1.480**	**6.1677**
FeP_5-a	C_s	2.537	3.000	0.975	7.604	2.156	5.448
FeP_5-b	C_1	2.364	3.000	0.625	7.511	2.240	5.275
FeP_5-c	C_s	2.480	3.000	0.799	7.817	2.133	5.684
FeP_5-d	C_s	2.391	3.000	0.934	7.782	2.044	5.738
FeP_5-e	**C_{5v}**	**2.663**	**3.000**	**1.240**	**8.327**	**1.7734**	**6.553**
FeP_6-a	**C_2**	**2.585**	**2.000**	**0.909**	**7.927**	**2.439**	**5.488**
FeP_6-b	C_{2v}	2.553	2.000	1.068	7.830	2.2099	5.621
FeP_6-c	C_s	2.573	4.000	0.871	7.603	2.1629	5.441
FeP_6-d	C_1	2.534	4.000	0.878	7.422	2.446	4.976
FeP_7-a	C_{3v}	2.452	1.000	0.671	6.925	1.608	5.317
FeP_7-b	C_1	2.597	1.000	0.968	7.609	2.457	5.152
FeP_7-c	**C_{3v}**	**2.608**	**1.000**	**1.029**	**7.542**	**2.274**	**5.268**
FeP_8-a	C_s	2.467	2.000	0.8739	7.472	2.406	5.066
FeP_8-b	**C_{2v}**	**2.677**	**2.000**	**1.234**	**7.561**	**1.910**	**5.652**
FeP_8-c	D_{4h}	2.661	2.000	0.852	8.084	2.807	5.277
FeP_8-d	C_1	2.599	2.000	0.820	7.564	2.312	5.253
FeP_8-e	C_1	2.512	2.000	0.926	7.805	2.642	5.163
FeP_9-a	C_1	2.492	3.000	0.394	7.578	2.963	4.616
FeP_9-b	C_1	2.570	1.000	0.758	7.852	2.969	4.883
FeP_9-c	C_1	2.532	3.000	0.698	7.502	2.483	5.018
FeP_9-d	C_s	2.569	3.000	0.799	7.627	3.047	4.580
FeP_9-e	C_{3v}	2.516	1.000	0.793	7.415	2.445	4.970
FeP_9-f	**C_1**	**2.640**	**3.000**	**0.983**	**8.019**	**2.784**	**5.235**
FeP_9-g	C_s	2.514	1.000	0.824	7.583	2.712	4.871
FeP_{10}-a	**C_1**	**2.590**	**4.000**	**1.105**	**7.549**	**2.920**	**4.629**
FeP_{10}-b	C_1	2.524	0.000	0.908	7.671	2.294	5.378
FeP_{10}-c	C_{2v}	2.498	2.000	0.801	7.497	3.090	4.407
FeP_{10}-d	C_1	2.464	2.000	0.477	7.458	3.082	4.374
FeP_{10}-e	C_1	2.527	2.000	0.638	7.645	3.049	4.596
FeP_{11}-a	C_s	2.497	3.000	0.633	7.367	2.937	4.430
FeP_{11}-b	C_1	2.547	1.000	0.674	7.749	3.04870	4.701
FeP_{11}-c	C_1	2.559	1.000	0.692	7.579	2.927	4.652
FeP_{11}-d	**C_1**	**2.663**	**3.000**	**0.971**	**7.486**	**2.886**	**4.600**
FeP_{11}-e	C_1	2.647	1.000	1.029	7.963	3.024	4.940
FeP_{11}-f	C_1	2.581	1.000	0.734	7.628	2.894	4.734
FeP_{12}-a	C_{6v}	2.501	2.000	1.101	7.522	2.457	5.065
FeP_{12}-b	C_1	2.548	2.000	0.693	7.536	3.159	4.378
FeP_{12}-c	C_{2v}	2.562	0.000	0.940	8.097	3.043	5.053
FeP_{12}-d	C_1	2.528	2.000	0.849	7.641	3.015	4.626
FeP_{12}-e	**C_1**	**2.624**	**2.000**	**0.997**	**7.602**	**2.972**	**4.630**
FeP_{12}-f	C_1	2.551	4.000	0.665	7.782	3.259	4.522
FeP_{13}-a	C_1	2.496	3.000	0.857	7.430	3.120	4.309
FeP_{13}-b	C_s	2.501	1.000	0.449	7.360	3.254	4.106
FeP_{13}-c	**C_1**	**2.611**	**1.000**	**0.714**	**7.756**	**3.210**	**4.456**
FeP_{13}-d	C_s	2.525	1.000	0.524	7.408	3.213	4.195
FeP_{13}-e	C_1	2.560	1.000	0.680	7.738	3.354	4.383
FeP_{14}-f	C_1	2.592	4.000	0.883	7.522	3.405	4.116
FeP_{14}-a	C_{2v}	2.561	0.000	0.810	7.589	3.039	4.550
FeP_{14}-b	**C_{2v}**	**2.629**	**2.000**	**0.799**	**8.005**	**3.550**	**4.454**
FeP_{14}-c	C_1	2.526	4.000	0.691	7.409	3.466	3.943
FeP_{14}-d	C_1	2.549	0.000	0.823	7.548	2.717	4.831

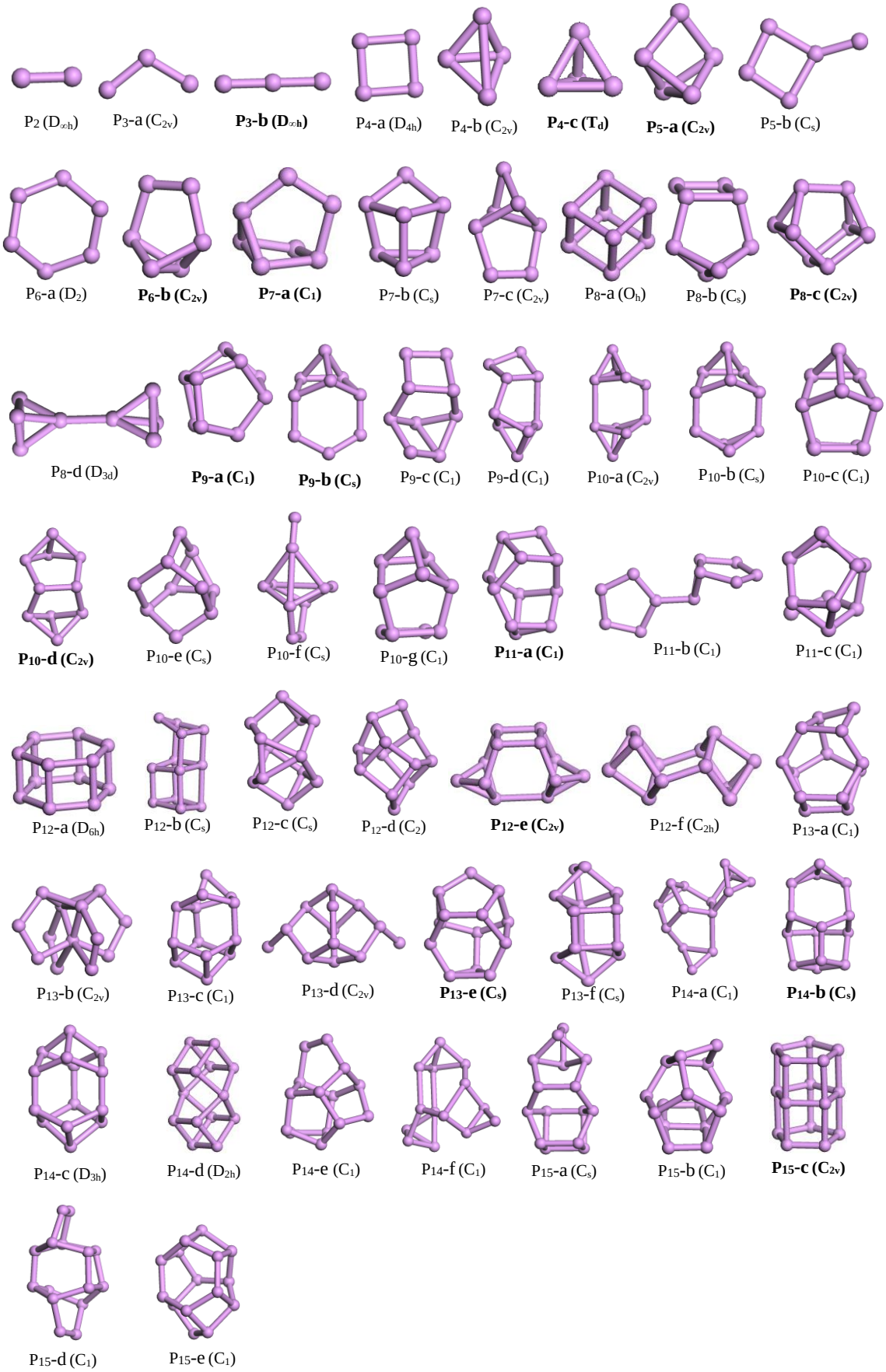

Fig. 1 Lowest energy structures and their corresponding isomers for P_{n+1} (n=1 -14) clusters. For each size, the lowest-energy isomers are reported in bold character

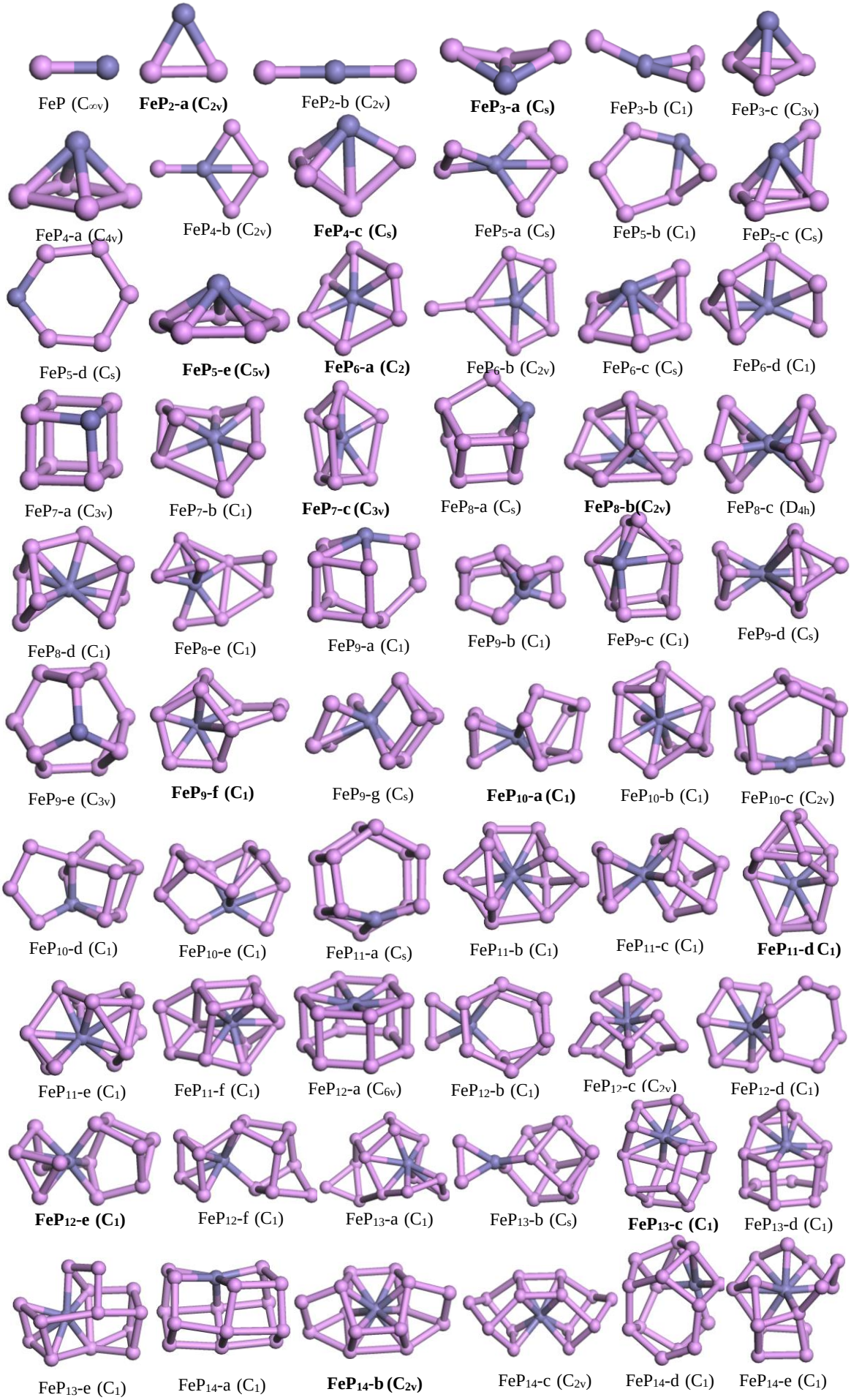

Fig. 2 Lowest energy structures and their corresponding isomers for FeP_n (n=1-14) clusters

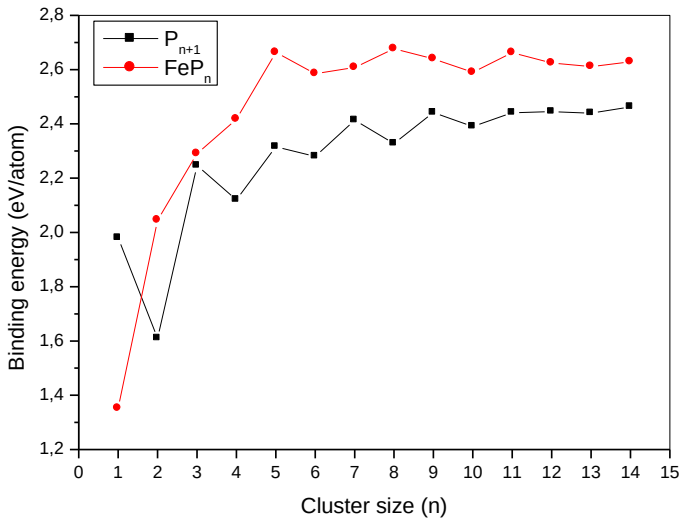

Fig. 3 Size dependence of binding energies per atom for the lowest energy structures of P_{n+1} and FeP_n (n = 1–14) clusters.

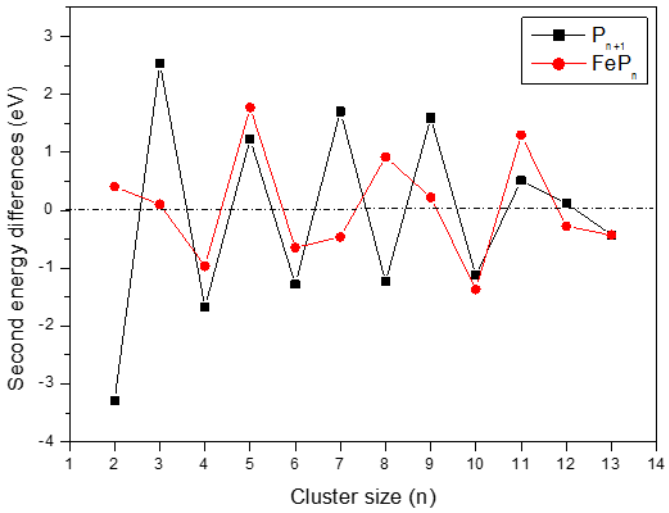

Fig. 4 Second-order difference of energies for the lowest energy structures of P_{n+1} and FeP_n (n = 1–14) clusters.

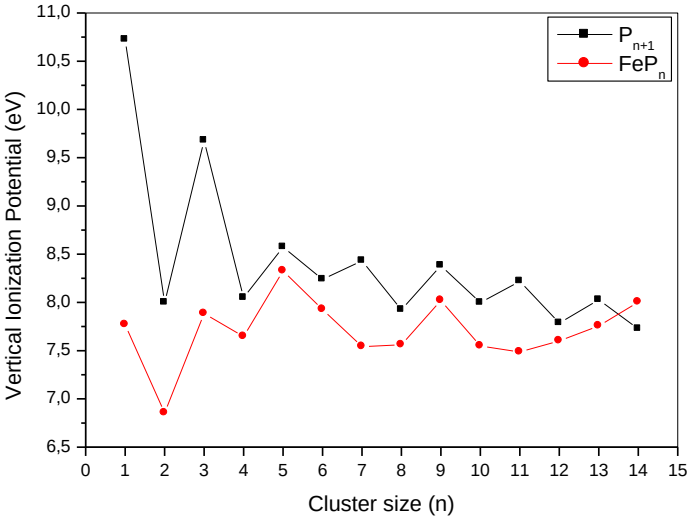

Fig. 5 Size dependence of the vertical ionization potential (VIP) for the lowest energy structures of P_{n+1} and FeP_n (n = 1–14) clusters.

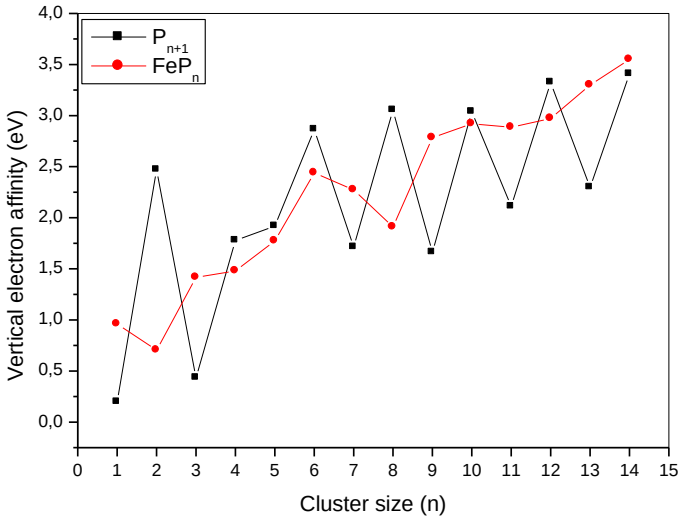

Fig. 6 Size dependence of the vertical electron affinity (VEA) for the lowest energy structures of P_{n+1} and FeP_n (n = 1–14) clusters.

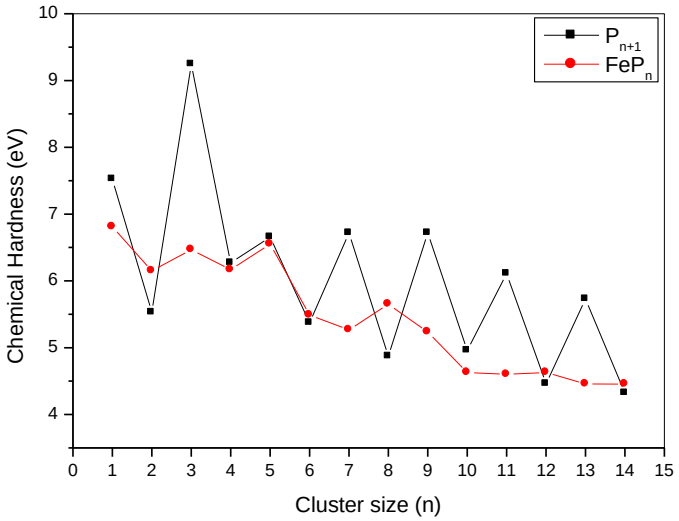

Fig. 7 Size dependence of the chemical hardness η for the lowest energy structures of P_{n+1} and FeP_n (n = 1–14) clusters.

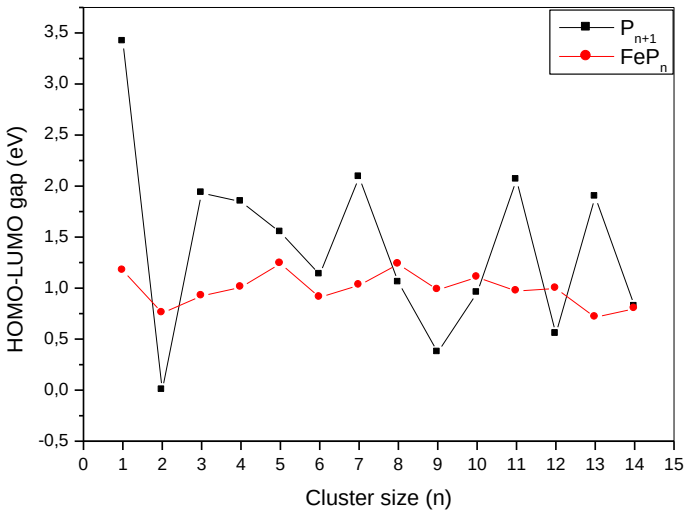

Fig. 8 Size dependence of HOMO-LUMO gap for the lowest energy structures of P_{n+1} and FeP_n (n = 1–14) clusters.

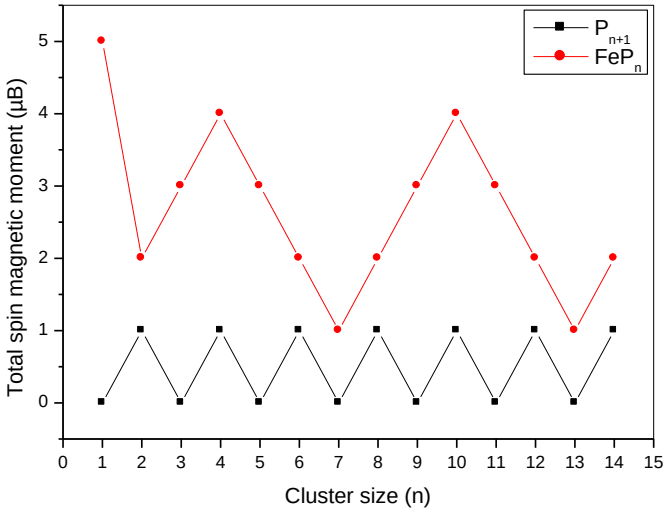

Fig. 9 Total spin magnetic moment for the lowest energy structures of P_{n+1} and FeP_n (n = 1-14) clusters.

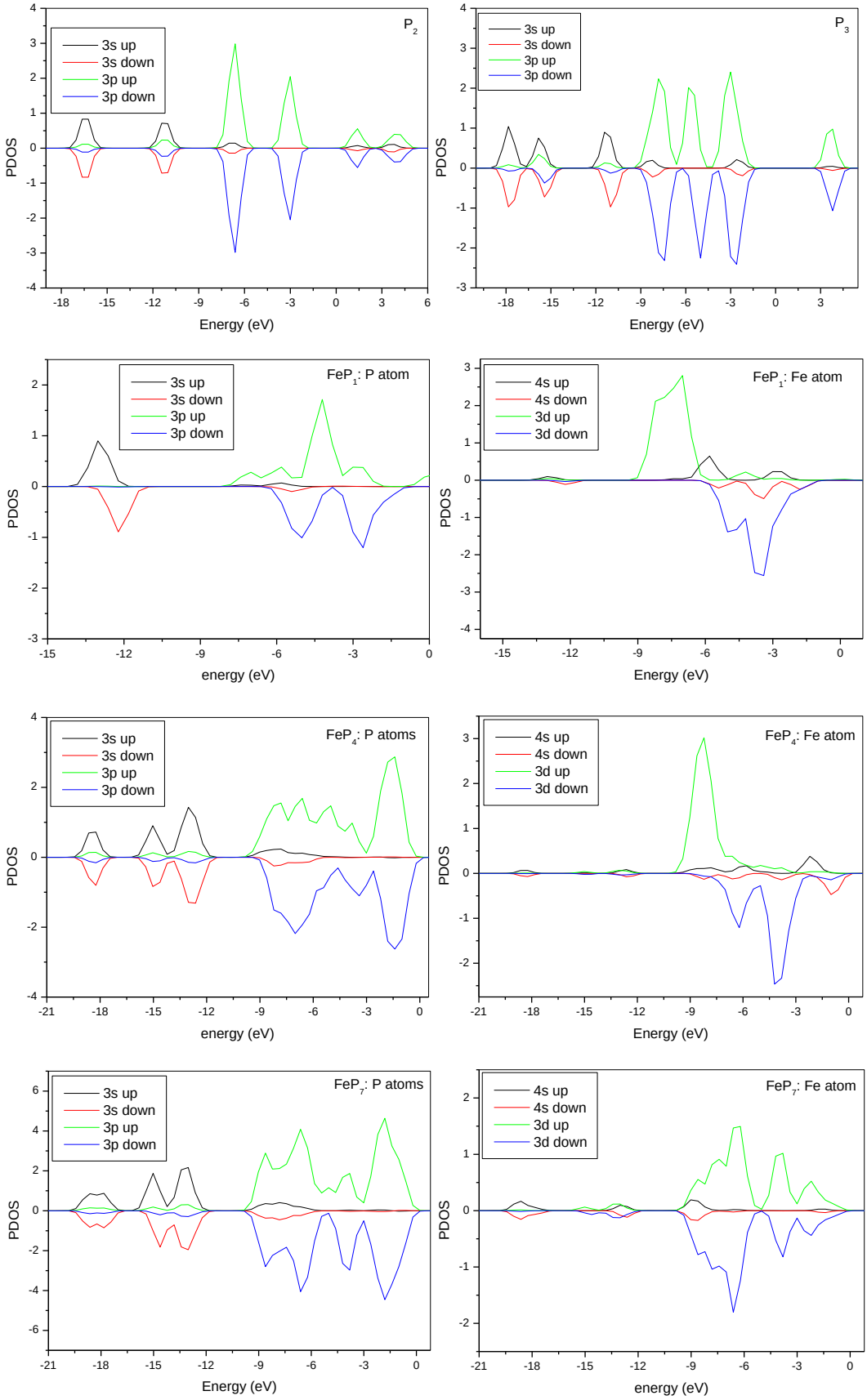

Fig. 10 The projected density of states (PDOS) for P_2, P_3, FeP_1, FeP_4 and FeP_7 clusters: contribution to the PDOS of P (left column) and Fe (right column) species.